



### International Conference on Medical Science, Medicine and Public Health

Hosted online from Jakarta, Indonesia

Website: econfseries.com 30<sup>th</sup> October, 2025

### COMPUTATIONAL STUDY OF A VERTICAL-AXIS LOW-POWER WIND TURBINE IN ANSYS FLUENT

<sup>1</sup>Музаффаров С.А., <sup>2</sup>Маратов Х.У., <sup>3</sup>Курбонова Г.Ф.

<sup>1</sup>Институт механики и сейсмостойкости сооружений им. М.Т. Уразбаева АН РУз, Ташкент, Узбекистан

<sup>2</sup>Бухарский государственный технический университет, Бухара, Узбекистан <sup>3</sup>Ташкентский университет информационных технологий имени Мухаммада ал-Хоразмий, Ташкент, Узбекистан

#### **Abstract**

In mathematical modeling of wind turbine aerodynamics within the ANSYS Fluent software package, the main problem is the choice of a turbulence model.

As part of the work, to describe the turbulent flow, the standard and modified  $k-\varepsilon$  models were tested, Spalart-Allmaras model,  $k-\omega$  model and RNG model for mixing description. The calculations used the control volume method embedded in ANSYS Fluent, where the velocity and pressure fields are linked by the PISO algorithm. Satisfactory agreement between the results of calculation and experiment was obtained when implementing the modified  $k-\varepsilon$  model according to the axial distributions of the longitudinal velocity. This model will be further used in determining the values of the tangential flow direction in the blades of the wind generator and the moment of its rotation.

**Keywords:** wind force, velocity field, Navier-Stokes equations, ANSYS Fluent, control volume method, PISO, turbulence models, computational experiment.

#### 1. INTRODUCTION

In recent years, the Republic of Uzbekistan has adopted a set of measures aimed at further increasing the efficiency of the use of electrical energy in the sectors of the economy and in everyday life, the widespread introduction of energy-saving technologies and the development of renewable energy sources.





### International Conference on Medical Science, Medicine and Public Health

Hosted online from Jakarta, Indonesia

Website: econfseries.com 30<sup>th</sup> October, 2025

Over the past 50 years, 85% of the electricity generation in the republic corresponds to natural gas. The carbon dioxide and carbon oxides emitted as a result of the combustion of hydrocarbons lead to atmospheric pollution, a decrease in its transparency and an increase in turbidity. This, in turn, enhances the "greenhouse effect", which over the past hundred years has increased the average temperature of the Earth's atmosphere by 1.5-2 degrees. Such global climate change leads to the melting of the glaciers of the north and south poles of the Earth, the frequent formation of anomalous climatic phenomena. Ultimately, this is reflected in the global ecological state of the planet and the development of civilization. In this regard, today the widespread use of alternative sources of electricity is becoming relevant [1-5].

Of the alternative sources of electricity, the cheapest and most environmentally appropriate is the driving force of the wind, which has a high economic indicator. In general, by 2030, the development of the total wind power capacity up to 5000 MW is predicted in Uzbekistan.

All this is about big energy. The government also supports small-scale power generation. Evidence of this judgment, in particular, is the financing, development and implementation of low-power wind turbines with a vertical axis of rotation.

The choice of a wind turbine with a vertical axis of rotation is justified by the fact that wind turbines with high power start working from 7 m/s wind speed. Such wind speeds in Central Asia are achieved at high altitudes, which is due to the areography of the area, or in certain regions, for example, in the Akhangaran valley, or in the coastal zones of the oceans. Thus, in the Republic of Uzbekistan, the wind potential refers to low wind speeds [6-10].

The second reason for choosing a wind turbine with a vertical axis of rotation is that such a design can operate with an arbitrary wind direction. When the wind direction changes, the horizontal axis of the wind turbine should be parallel to the wind direction. This is achieved either automatically, which requires additional capital investments, or manually, which requires additional operating costs.

Currently, software products are actively used in scientific and technical organizations and universities for modeling various processes. Their use in the study





### International Conference on Medical Science, Medicine and Public Health

Hosted online from Jakarta, Indonesia

Website: econfseries.com 30<sup>th</sup> October, 2025

of heat engineering processes observed in engineering and technology has become relevant.

Most of the world's leading companies use ANSYS products. The complexes present the widest range of modern physical models, and it is also possible to carry out multidisciplinary calculations within the framework of the ANSYS Workbench integrating environment. With a friendly user interface and robust solvers, ANSYS CFD products can be mastered in a short amount of time. The integration of ANSYS CFD into the ANSYS Workbench environment and the unified ANSYS CFD-Post post-processor combine to create the most complete simulation suite available to the engineering community. ANSYS CFD is fully integrated into the ANSYS Workbench environment, which is an engineering simulation framework, and all ANSYS tools and software packages are integrated into it. This adaptive architecture allows users to easily create models ranging from fluid dynamics problems to complex multiphysics system interactions with simple drag and drop operations. Users can easily evaluate product performance at multiple design points or compare a range of alternative concepts.

In the process of solving the problem, the following turbulence models are used to describe turbulence.

The complete system of Navier-Stokes equations with two, one (Spalart-Almars model) or non-linear diffusion equations that take into account fluctuations in the average velocity of turbulent flows is a family of models  $k-\varepsilon$  and  $k-\omega$ , where k turbulent energy mass density;  $\varepsilon$  – its dissipation rate;  $\omega$  – energy dissipation rate per unit volume and time. A feature of this system is the cascading of its solution, which is most convenient for use in software packages for modeling processes in cylindrical coordinates.

ANSYS CFD has the widest variety of turbulence models available, including the time-tested k- $\epsilon$ , k- $\omega$ , and Reynolds Stress Model (RSM) for highly swirling or anisotropic flows. Due to the ever-increasing performance of computers and decreasing their cost, large eddy models (LES) and more economical non-attached eddy models (DES) have become extremely popular in solving industrial problems. New innovative models that allow calculation of the laminar-turbulent transition and a modern model (SAS) that automatically determines the scale of turbulent eddies





### International Conference on Medical Science, Medicine and Public Health

Hosted online from Jakarta, Indonesia

Website: econfseries.com 30<sup>th</sup> October, 2025

are usually used in cases where the accuracy of stationary turbulence models is not enough. Various near-wall functions and the enhanced wall treatment method make it possible to describe the flows bounded by walls as accurately as possible [6]. In the process of solving the problem, five turbulence models can be used to describe turbulence.

#### 2. METHOD.

Model modified  $k-\varepsilon$ . In contrast to the well-known works, it is proposed here to describe the turbulent exchange using a modified  $k-\varepsilon$  model, which contributes to a more adequate description of the heat and mass transfer process:

$$\begin{split} &\left[\frac{\partial}{\partial t}(\rho k) + \frac{\partial}{\partial x_{j}}(\rho k u_{j}) = \frac{\partial}{\partial x_{j}}\left[\left(\mu + \frac{\mu_{t}}{\sigma_{k}}\right)\frac{\partial k}{\partial x_{j}}\right] + G_{k} + G_{b} - \rho\varepsilon - 2\rho\varepsilon M_{t}^{2} + S_{k}, \\ &\left[\frac{\partial}{\partial t}(\rho\varepsilon) + \frac{\partial}{\partial x_{j}}(\rho\varepsilon u_{j}) = \frac{\partial}{\partial x_{j}}\left[\left(\mu + \frac{\mu_{t}}{\sigma_{\varepsilon}}\right)\frac{\partial\varepsilon}{\partial x_{j}}\right] + \rho C_{1}S\varepsilon - \rho C_{2}\frac{\varepsilon^{2}}{k + \sqrt{\nu\varepsilon}} + C_{1\varepsilon}\frac{\varepsilon}{k}C_{3\varepsilon}G_{b} + S_{\varepsilon}. \end{split}$$

Here we use the notation

$$C_{1} = \max \left[ 0.43, \frac{\eta}{\eta + 5} \right], \quad \eta = S \frac{k}{\varepsilon}, \quad S = \sqrt{2S_{ij}S_{ij}}, \quad \mu_{t} = \rho C_{\mu} \frac{k^{2}}{\varepsilon}, \quad C_{\mu} = \frac{1}{A_{0} + A_{S} \frac{kU^{*}}{\varepsilon}}, \quad U^{*} \equiv \sqrt{S_{ij}S_{ij} + \tilde{\Omega}_{ij}} \tilde{\Omega}_{ij}$$

$$, \quad \Omega_{ij} = \overline{\Omega_{ij}} - 2\varepsilon_{ijk}\omega_{k}, \quad A_{S} = \sqrt{6}\cos\phi, \quad \phi = \frac{1}{3}\cos^{-1}\left(\sqrt{6}W\right), \quad W = \frac{S_{ij}S_{jk}S_{ki}}{\tilde{S}^{3}}, \quad \tilde{S} = \sqrt{S_{ij}S_{ij}},$$

$$S_{ij} = \frac{1}{2}\left(\frac{\partial u_{j}}{\partial x_{i}} + \frac{\partial u_{i}}{\partial x_{j}}\right), \quad G_{k} = -\rho \overline{u_{i}'u_{j}'} \frac{\partial u_{j}}{\partial u_{i}}, \quad S \equiv \sqrt{2S_{ij}S_{ij}}, \quad G_{b} = \beta g_{i} \frac{\mu_{t}\partial T}{\Pr_{t}\partial x_{i}}, \quad \Pr_{t} = 1/a_{t},$$

$$a_{0} = 1/\Pr_{t} = k/\mu c_{p}, \quad \beta = -\frac{1}{2}\left(\frac{\partial \rho}{\partial T}\right), \quad G_{b} = -g_{i} \frac{\mu_{t}}{\rho \Pr_{t}} \frac{\partial \rho}{\partial x_{i}}, \quad M_{t} = \sqrt{\frac{k}{a^{2}}}, \quad a = \sqrt{\gamma RT}.$$

Empirical Constants  $k-\varepsilon$  models take standard values:  $C_{1\varepsilon} = 1.44$ ,  $C_2 = 1.9$ ,  $\sigma_k = 1.0$ ,  $\sigma_{\varepsilon} = 1.2$ ,  $A_0 = 4.04$ .

Spalart-Allmaras model. This model belongs to the class of one-parameter linear turbulence models. Here, only one additional differential equation appears for calculating the kinematic coefficient of eddy viscosity. This low Reynolds turbulence model, which describes the entire flow region, is given by the following equation:





### International Conference on Medical Science, Medicine and Public Health

Hosted online from Jakarta, Indonesia

Website: econfseries.com 30<sup>th</sup> October, 2025

$$\frac{\partial}{\partial t} (\rho \tilde{v}) + \frac{\partial}{\partial x_i} (\rho \tilde{v} u_i) =$$

$$G_{v} + \frac{1}{\sigma_{\tilde{v}}} \left[ \frac{\partial}{\partial x_{j}} \left\{ \left( \mu + \rho \tilde{v} \right) \frac{\partial \tilde{v}}{\partial x_{j}} \right\} + C_{b2\rho} \left( \frac{\partial \tilde{v}}{\partial x_{j}} \right)^{2} \right] - C_{w1\rho} f_{w} \left( \frac{\tilde{v}}{d} \right)^{2} + S_{\tilde{v}}.$$

Turbulent eddy viscosity is calculated by the formule:  $\mu_t = \rho \tilde{v} f_{v_1}$ , additional definitions are given by the following dependencies:  $f_{v_1} = \frac{\chi^3}{\chi^3 + C^3}$ ,  $\chi = \frac{\tilde{v}}{v}$ 

$$\tilde{S} \equiv S + \frac{v}{\kappa^2 d^2} f_{v2}, \qquad f_{v2} = 1 - \frac{\chi}{1 + \chi f_{v1}}, \\ S \equiv \sqrt{2\Omega_{ij}\Omega_{ij}}, \qquad \Omega_{ij} = \frac{1}{2} \left( \frac{\partial u_i}{\partial x_j} - \frac{\partial u_j}{\partial x_i} \right), \qquad S_{ij} = \frac{1}{2} \left( \frac{\partial u_j}{\partial x_i} + \frac{\partial u_i}{\partial x_j} \right),$$

 $f_w = g \left[ \frac{1 + C_{w3}^6}{g^6 + C_{w3}^6} \right]^{1/6}$ ,  $r = \frac{\tilde{v}}{\tilde{S}\kappa^2 d^2}$ , and the closure constants for the model:  $C_{prod} = 2.0$ ,

$$C_{b1} = 0.1355 C_{b2} = 0.622, \quad \sigma_{\tilde{v}} = \frac{2}{3}, \quad C_{v1} = 7.1, \quad C_{w1} = \frac{C_{b1}}{\kappa^2} + \frac{(1 + C_{b2})}{\sigma_{\tilde{v}}}, \quad C_{w2} = 0.3 C_{w3} = 2.0,$$

 $\kappa = 0.4187$ .

Standard model  $k - \varepsilon$ .

$$\begin{cases} \frac{\partial}{\partial t}(\rho k) + \frac{\partial}{\partial x_{i}}(\rho k u_{i}) = \frac{\partial}{\partial x_{j}} \left[ \left( \mu + \frac{\mu_{t}}{\sigma_{k}} \right) \frac{\partial k}{\partial x_{j}} \right] + G_{k} + G_{b} - \rho \varepsilon - Y_{M} + S_{k}, \\ \frac{\partial}{\partial t}(\rho \varepsilon) + \frac{\partial}{\partial x_{i}}(\rho \varepsilon u_{i}) = \frac{\partial}{\partial x_{j}} \left[ \left( \mu + \frac{\mu_{t}}{\sigma_{\varepsilon}} \right) \frac{\partial \varepsilon}{\partial x_{j}} \right] + \\ + C_{1\varepsilon} \frac{\varepsilon}{k} \left( G_{k} + C_{3\varepsilon} G_{b} \right) - C_{2\varepsilon\rho} \frac{\varepsilon^{2}}{k} + S_{\varepsilon}. \end{cases}$$

Turbulent eddy viscosity is calculated by the formula:  $\mu_t = \rho C_{\mu} \frac{k^2}{\varepsilon}$ , closure constants for standard  $k - \varepsilon$  models:  $C_{1\varepsilon} = 1.44$ ,  $C_{2\varepsilon} = 1.92$ ,  $C_{\mu} = 0.09$ ,  $\sigma_k = 1.0$ ,  $\sigma_{\varepsilon} = 1.3$ . Model RNG  $k - \varepsilon$  [10-12].





### International Conference on Medical Science, Medicine and Public Health

Hosted online from Jakarta, Indonesia

Website: econfseries.com 30<sup>th</sup> October, 2025

$$\begin{cases} \frac{\partial}{\partial t}(\rho k) + \frac{\partial}{\partial x_{i}}(\rho k u_{i}) = \frac{\partial}{\partial x_{j}}\left(\alpha_{k}\mu_{eff}\frac{\partial k}{\partial x_{j}}\right) + G_{k} + G_{b} - \rho\varepsilon - Y_{M} + S_{k}, \\ \frac{\partial}{\partial t}(\rho\varepsilon) + \frac{\partial}{\partial x_{i}}(\rho\varepsilon u_{i}) = \frac{\partial}{\partial x_{j}}\left(\alpha_{\varepsilon}\mu_{eff}\frac{\partial\varepsilon}{\partial x_{j}}\right) + \\ + C_{1\varepsilon}\frac{\varepsilon}{k}(G_{k} + C_{3\varepsilon}G_{b}) - C_{2\varepsilon\rho}\frac{\varepsilon^{2}}{k} - R_{\varepsilon} + S_{\varepsilon}. \end{cases}$$

Turbulent eddy viscosity is calculated by the formula:  $\mu_t = \rho C_\mu \frac{k^2}{\varepsilon}$ , closure constants

for RNG 
$$k - \varepsilon$$
 models:  $C_{\mu} = 0.0845$ ,  $R_{\varepsilon} = \frac{C_{\mu} \rho \eta^3 (1 - \eta / \eta_0)}{1 + \beta \eta^3} \frac{\varepsilon^2}{k}$ ,  $\eta = Sk / \varepsilon$ ,  $\eta_0 = 4.38$ ,

$$\beta = 0.012, \ \eta \approx 3.0, \ C_{2\varepsilon}^* \approx 2.0, \ C_{1\varepsilon} = 1.42, \ C_{2\varepsilon} = 1.68.$$

Model  $k-\omega$  - historically the very first High Reynolds model with two differential equations [12-14]:

$$\left\{ \frac{\partial}{\partial t} (\rho k) + \frac{\partial}{\partial x_i} (\rho k u_i) = \frac{\partial}{\partial x_j} \left[ \Gamma_k \frac{\partial k}{\partial x_j} \right] + G_k - \rho \beta^* f_{\beta^*} k \omega + S_k, 
\left\{ \frac{\partial}{\partial t} (\rho \omega) + \frac{\partial}{\partial x_i} (\rho \omega u_i) = \frac{\partial}{\partial x_j} \left[ \Gamma_\omega \frac{\partial \omega}{\partial x_j} \right] + G_\omega - \rho \beta f_\beta \omega^2 + S_\omega. \right\}$$

Does not contain terms reflecting the effect of molecular viscosity on turbulence. Now rarely used.

Turbulent eddy viscosity is calculated by the formula:  $\mu_t = \alpha^* \frac{\rho k}{\omega}$ , model inserts are

defined as a function 
$$\Gamma_k = \mu + \frac{\mu_t}{\sigma_k}$$
,  $\Gamma_\omega = \mu + \frac{\mu_t}{\sigma_\omega}$ ,  $\alpha^* = \alpha_\infty^* \left( \frac{\alpha_0^* + \operatorname{Re}_t / R_k}{1 + \operatorname{Re}_t / R_k} \right)$ ,  $\operatorname{Re}_t = \frac{\rho k}{\mu \omega}$ ,

$$G_{k} = -\rho \overline{u'_{i}u'_{j}} \frac{\partial u_{j}}{\partial x_{i}}, \quad \Omega_{ij} = \frac{1}{2} \left( \frac{\partial u_{i}}{\partial x_{i}} - \frac{\partial u_{j}}{\partial x_{i}} \right), \quad G_{\omega} = \alpha \frac{\omega}{k} G_{k}, \quad \alpha = \frac{\alpha_{\omega}}{\alpha^{*}} \left( \frac{\alpha_{0} + \operatorname{Re}_{t} / R_{\omega}}{1 + \operatorname{Re}_{t} / R_{\omega}} \right), \quad \chi_{k} \equiv \frac{1}{\omega^{3}} \frac{\partial k}{\partial x_{j}} \frac{\partial \omega}{\partial x_{j}},$$

$$\beta^* = \beta_i^* [1 + \zeta^* F(M_t)],$$
 closure constants for model  $k - \omega$ :  $\alpha_0^* = \frac{\beta_i}{3},$   $R_k = 6,$ 





### International Conference on Medical Science, Medicine and Public Health

Hosted online from Jakarta, Indonesia

Website: econfseries.com 30<sup>th</sup> October, 2025

$$\beta_i = 0.072, \ \alpha^* = \alpha_{\infty}^* = 1, \ R_{\omega} = 2.95, \ \alpha = \alpha_{\infty} = 1, \ \beta_i^* = \beta_{\infty}^* \left( \frac{4/15 + \left( \operatorname{Re}_t / R_{\beta} \right)^4}{1 + \left( \operatorname{Re}_t / R_{\beta} \right)^4} \right), \ \zeta^* = 1.5$$

$$, R_{\beta} = 8, \beta_{\infty}^{*} = 0.09, \chi_{\omega} = \left| \frac{\Omega_{ij} \Omega_{ij} S_{ij}}{\left(\beta_{\infty}^{*} \omega\right)^{3}} \right|, \beta = \beta_{i} \left[ 1 - \frac{\beta_{i}^{*}}{\beta_{i}} \zeta^{*} F(M_{t}) \right], M_{t}^{2} = \frac{2k}{a^{2}}, M_{t0} = 0.25,$$

$$a = \sqrt{\gamma RT} , \quad \alpha_{\infty}^* = 1, \quad \alpha_{\infty} = 0.52, \quad \alpha_{0} = \frac{1}{9}, \quad \beta_{\infty}^* = 0.09, \quad \beta_{i} = 0.072, \quad R_{\beta} = 8, \quad R_{k} = 6,$$
 
$$R_{\omega} = 2.95, \quad \zeta^* = 1.5, \quad M_{t0} = 0.25, \quad \sigma_{k} = 2.0, \quad \sigma_{\omega} = 2.0.$$

### **Rotating machines [8]**

ANSYS CFD has been the leading CFD software for modeling rotating machines for many years. It is a leader in the field, where the requirements for accuracy, speed and stability of the calculation are extremely high. ANSYS CFD combines a complete set of models, end-to-end analysis of stationary and rotating turbomachinery components, and specialized add-ons for easy preparation and analysis of mechanical engineering problems. All this makes the complex the most complete and meets the requirements of calculation engineers. The ANSYS family of complexes contains the ANSYS BladeModeler and ANSYS TurboGrid modules for quick and easy creation of a geometric model of a blade wheel and the construction of a high-quality hexahedral computational grid.

The paper considers a variant of the problem of modeling the flow around the developed wind turbine.

### Geometry of the object under study

The construction of the CAD model (Fig. 1.) was carried out in the SolidWorks environment, where the main geometric dimensions were specified. Since the task is reduced to modeling a flat task, the 2D design mode was chosen.





### International Conference on Medical Science, Medicine and Public Health

Hosted online from Jakarta, Indonesia

Website: econfseries.com 30<sup>th</sup> October, 2025

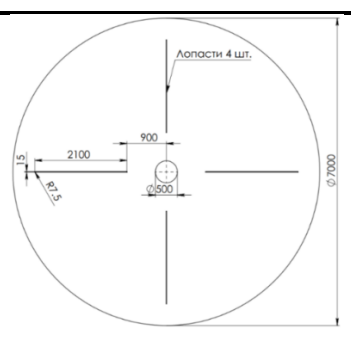


Figure 1. Geometry of a 2D four-bladed wind turbine (top view)

### Calculation grid

Next, the CAD model was exported to the Cadence Pointwise program to create a hybrid finite volume mesh (Fig. 2). An O-grid topology type was chosen to define the CFD flow domain. The input velocity boundary condition was specified in the I first quarter of the circular domain and in the remaining parts of the atmospheric pressure output condition. Also, layers of cells were allowed directly at the walls of the blades for accurate modeling of the turbulent viscous layer, where Y+<4.

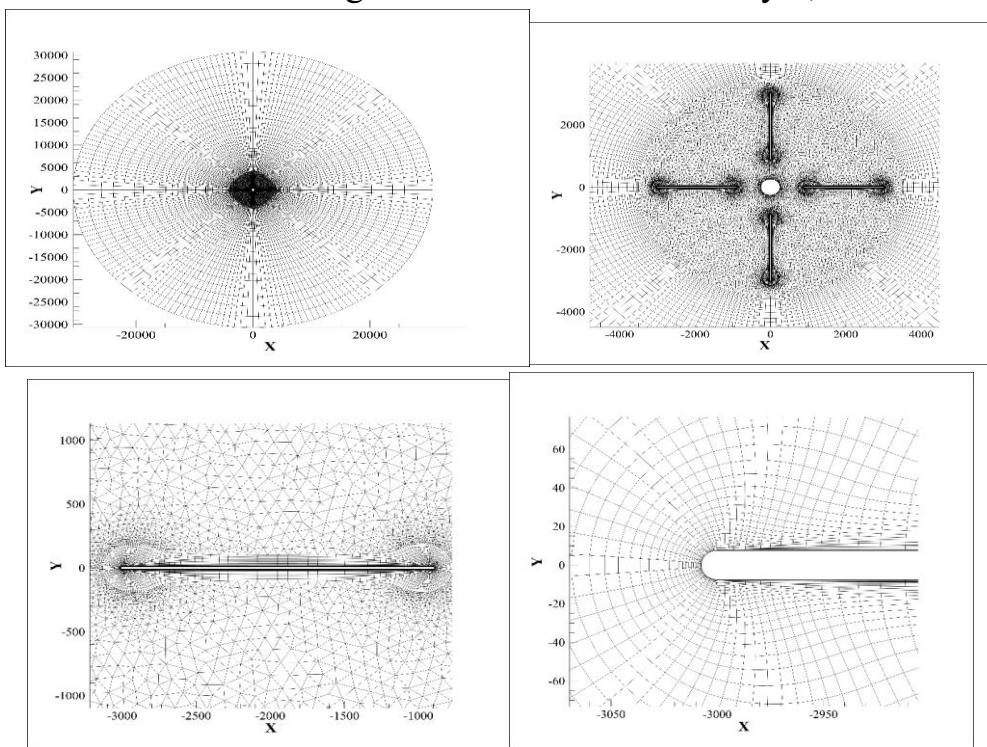


Figure 2. Unstructured computational grid of finite volumes





#### International Conference on Medical Science, Medicine and Public Health

Hosted online from Jakarta, Indonesia

Website: econfseries.com 30<sup>th</sup> October, 2025

### **Ansys Fluent Dynamic Mesh**

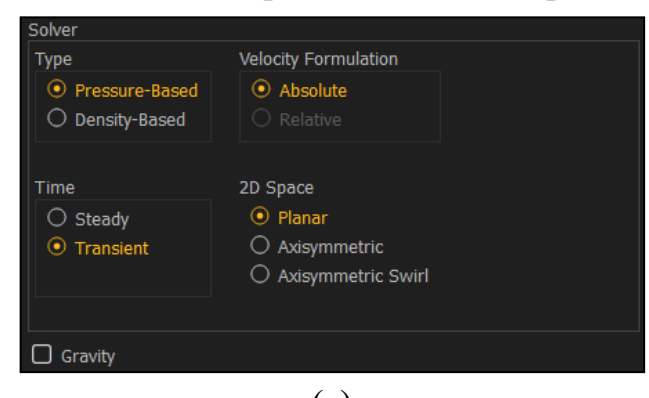
Ansys Fluent is a general purpose computational fluid dynamics (CFD) software used to simulate fluid flow, heat and mass transfer, chemical reactions, and more. Fluent offers a modern, user-friendly interface that streamlines the CFD process from pre-processing to post-processing in a single-window workflow.

The main advantage of this program is that Fluent allows you to use Dynamic Mesh technology for tasks with a dynamic mesh. The dynamic grid model allows you to move cell zone boundaries relative to other zone boundaries and adjust the grid accordingly. Boundary motion can be rigid, such as pistons moving inside an engine cylinder or flap, deviating on an aircraft wing, or deforming, such as the elastic wall of a balloon during inflation, or the flexible wall of an artery responding to a pressure impulse from the heart. In any case, the nodes that determine that the cells in the domain must be updated based on time, and hence the dynamic grid solutions are inherently non-stationary.

Solver settings and post-processing

Type - unsteady incompressible flow in 2D formulation (Fig. 4.5a). The mass of the installation is 68 kg, the moment of inertia along the Z axis is 85 kg·m<sup>2</sup> (Fig. 3). Input speed – V = 5 m/s.

To describe turbulence in the first version, a two-parameter low-Reynolds Menter model was chosen  $k-\omega$  SST (Fig. 4.5 c). The pressure-velocity coupled scheme was chosen by Coupled, which provides the best time convergence. Spatial discretization is second order for all quantities. Time step  $t=0.01\,c$ .



(a)





### International Conference on Medical Science, Medicine and Public Health

Hosted online from Jakarta, Indonesia

Website: econfseries.com 30<sup>th</sup> October, 2025

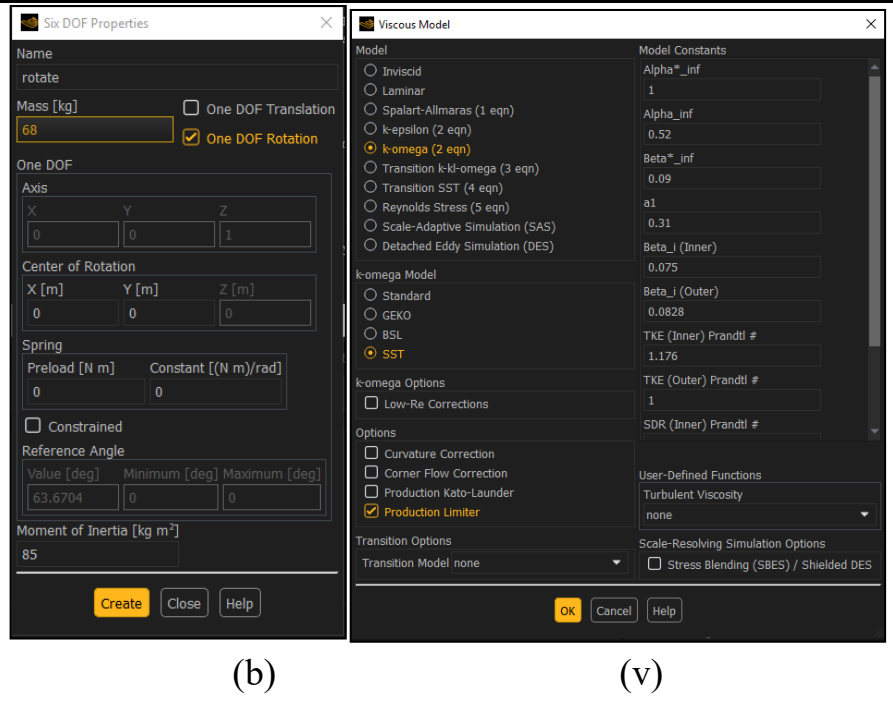


Figure 3. Model settings interface

### Calculation algorithm

The equations described above are integrated by the finite volume method in the ANSYS Fluent package. Convective and diffusion flows are calculated with the second order of approximation. Due to the fact that all the problems modeled below are quasi-stationary, the first order of approximation in time is used. The velocity and pressure fields are linked by the PISO algorithm. Solution algorithms, depending on the selected combustion model, have distinctive features.

#### 3. RESULTS AND DISCUSSION.

The results of modeling the rotation of the wind turbine blades showed a speed of 20-25 rpm at a wind speed of 5 m/s (see Fig. 4). A calculation was also carried out for the case of 8 m/s (see Fig. 5).





### International Conference on Medical Science, Medicine and Public Health

Hosted online from Jakarta, Indonesia

Website: econfseries.com 30<sup>th</sup> October, 2025

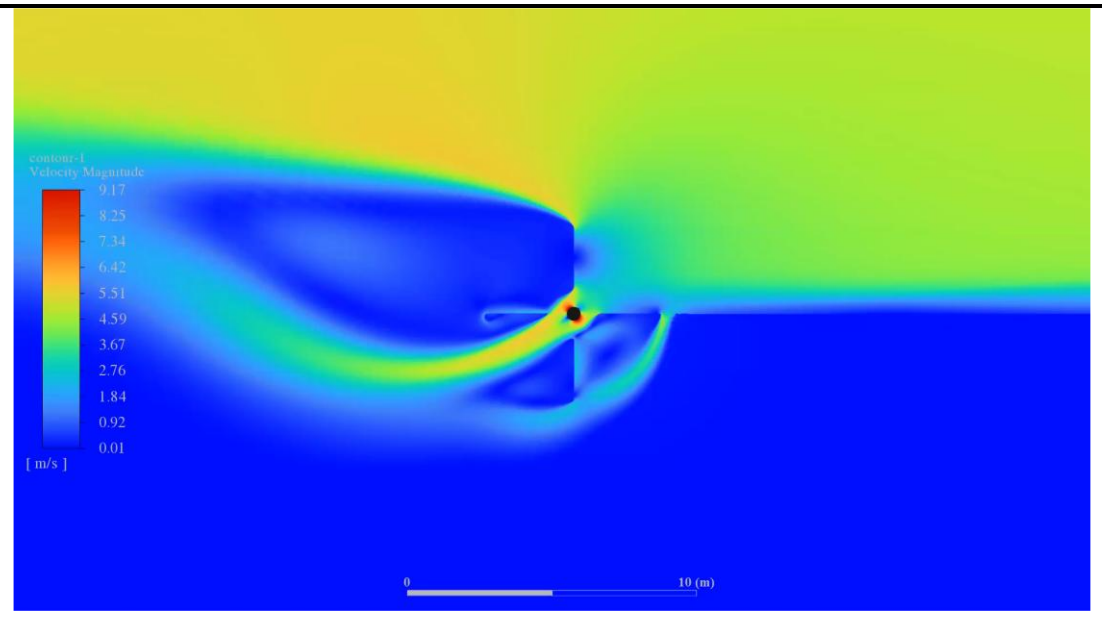


Figure 4. Contour of rotation speed V=5 m/s. K-ω model

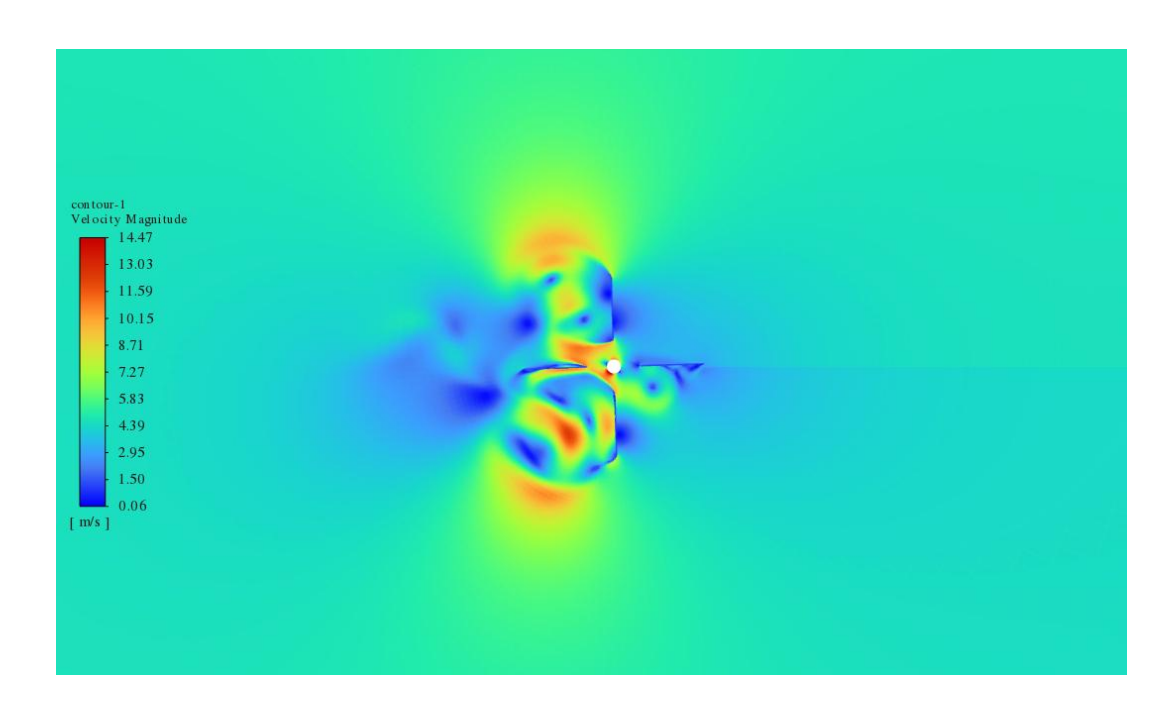


Figure 5. Contour of rotation speed V=8 m/s.  $K-\omega$  model





### International Conference on Medical Science, Medicine and Public Health

Hosted online from Jakarta, Indonesia

Website: econfseries.com 30<sup>th</sup> October, 2025

Calculations were also carried out using  $k - \varepsilon$  turbulence models (Fig. 6) and other turbulence models.

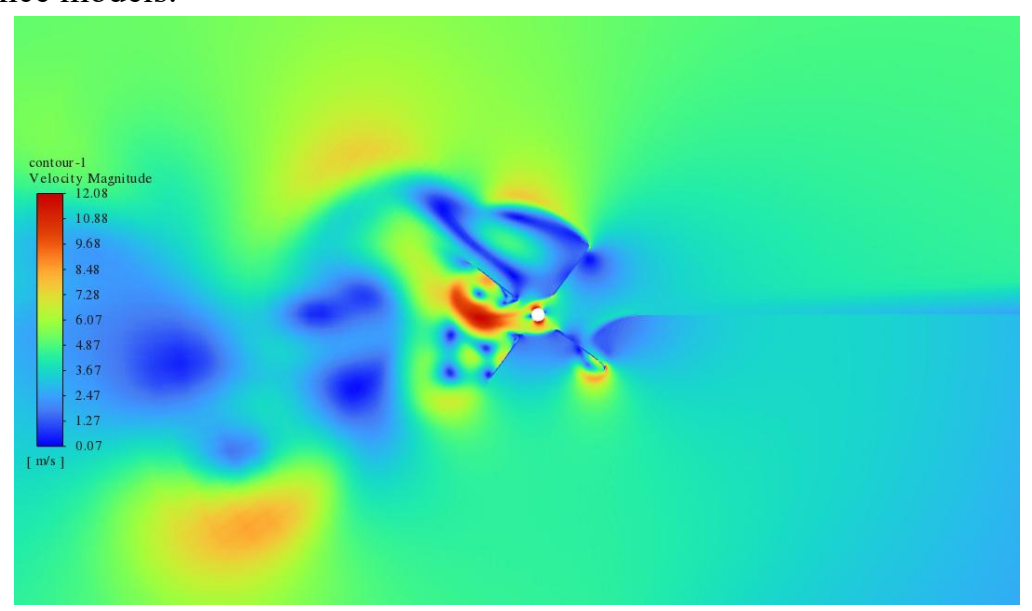


Figure 6. Contour of rotation speed V=5 m/s.  $k-\varepsilon$  model

The results of calculating the drag coefficient from the angular position of the first blade using the  $k-\varepsilon$  turbulence model are compared with experimental data (Fig. 7).

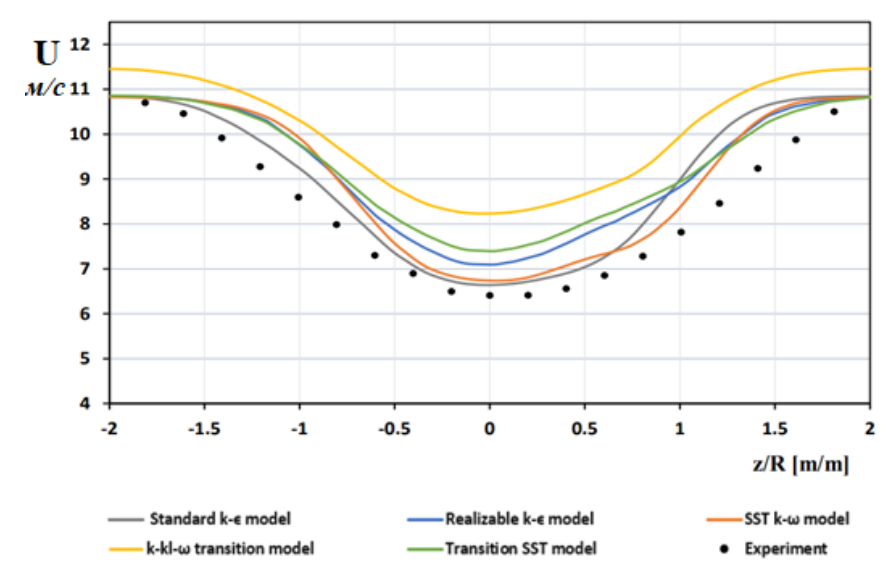


Figure 7 Axial Velocity Profile on a Vertical Line at Hub Height





### International Conference on Medical Science, Medicine and Public Health

Hosted online from Jakarta, Indonesia

Website: econfseries.com 30<sup>th</sup> October, 2025

A comparison of the experimentally determined profile of the axial velocity on a vertical line at the height of the hub with the profiles obtained with different turbulence models showed that it is desirable to use models  $k-\omega$  and  $k-\varepsilon$  in this regard.

According to the preliminary experimental results, the power curve of the installation was constructed depending on the wind speed (Fig. 8).

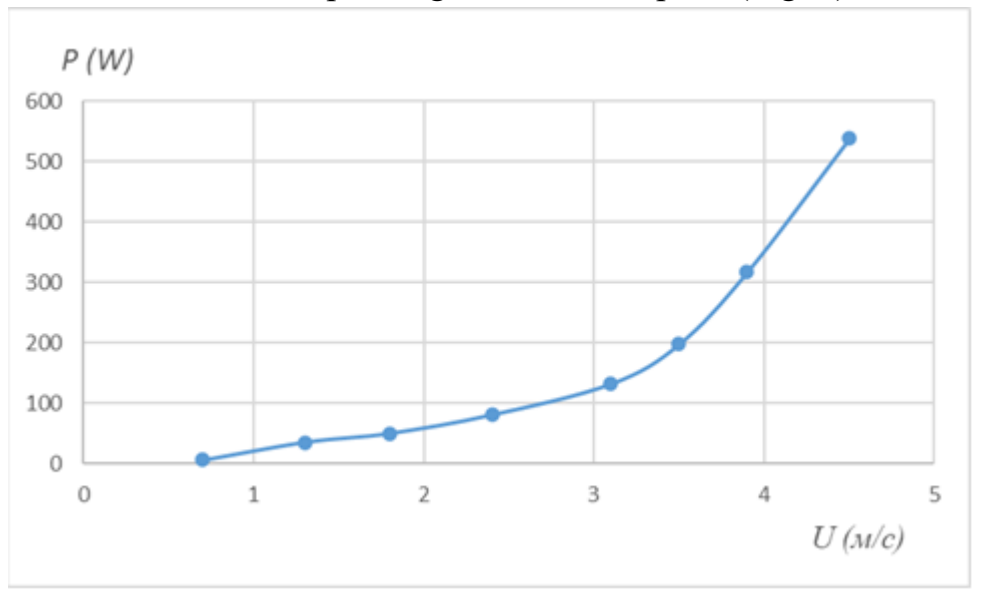


Figure 8. Power Curve

Numerous results on the aerodynamics of a wind turbine with a vertical axis of rotation have been obtained, which should be further processed by statistical methods and analyzed.

#### **CONCLUSIONS**

Theoretical calculations in the ANSYS environment have established that when calculating the aerodynamics of the proposed low-power wind generator, turbulence models  $k-\omega$  and  $k-\varepsilon$  can be used, which more adequately describe the process of flow around a rotating device.

Initial experimental results have been obtained, showing that at wind speeds above 4-5 m/s, the developed device can provide 0.7 kW of energy. The results on wind





### International Conference on Medical Science, Medicine and Public Health

Hosted online from Jakarta, Indonesia

Website: econfseries.com 30<sup>th</sup> October, 2025

turbine aerodynamics, which are not included in this report, must be further processed by statistical methods and analyzed.

#### REFERENCES

- 1. Toirov O.Z., Alimkhodzhaev K.T., Alimkhodzhaev Sh.K. Kaita tiklanuvchi is the energy of manbalari. Uzbekiston Sharoitida ishlab chiqarish va ishlatish istiqbollari.— T.: "Fan va texnologiya", 2019.—212
- 2. Solovyov Alexander, Degtyarev Kirill. Wind energy // Science and life. 2013. No. 7. P. 42.
- 3. Energy portal. Issues of production, conservation and processing of energy. Retrieved: 1 April 2022
- 4. Obukhov S.G. Electricity Generation Systems Using Renewable Energy Resources: Textbook. Publishing House of Tomsk State University, 2008. 150 p.
- 5. Martyanov A.S. Research of control algorithms and development of a controller for a wind power plant with a vertical axis of rotation: diss ... cand. tech. Sciences. Chelyabinsk, 2016. 174 p.
- 6. Mezaal N.A. Mathematical modeling of a wind power plant (WPP) with a capacity of 1.5 MW using computational fluid dynamics (CFD) in ANSYS: Master's thesis. Chelyabinsk: SUSU, 2018. 100 p.
- 7. Pavlenko I.M. Sovershenstvovaniye sistemi generirovaniya elektroenergii na osnove multimodulnoy vetroelektrostansii: avtoreferat diss... kand. texn. nauk. Saratov, 2013. 20 s.
- 8. Belyakov P.Yu., Ryabov D.Yu. Matematicheskaya model dlya issledovaniya xarakteristik i rejimov raboti vetroenergeticheskoy ustanovki s krilchatim vetropri yemnikom // Jurnal «Elektrotexnicheskiye kompleksi i sistemi upravleniya», www. v-itc.ru/electrotech. 6 s.
- 9. Oganesyan E.V., Bekirov E.A., Asanov M.M. Matematicheskaya model dlya opredeleniya parametrov raboti vetroenergeticheskoy ustanovki // Stroitelstvo i tex nogennaya bezopasnost, №3 (55), 2016. S. 82-86.
- 10. Kaplya Ye.V. Matematicheskaya model perexodnix protsessov povorotno opastnoy





### International Conference on Medical Science, Medicine and Public Health

Hosted online from Jakarta, Indonesia

Website: econfseries.com 30<sup>th</sup> October, 2025

vetroenergeticheskoy ustanovki // Matem. modelirovaniye, 2013, tom 25, №12. – S. 33–43.

- 11. Chernotalova Ye.A. Razrabotka vetrovoy elektrostansii dlya promishlennog o predpriyatiya g. Tolyatti: magisterskaya dissertatsiya. Tolyattinskiy Gosudarstvenniy universitet, 2019. 79 s.
- 12. Velkin V.I. Energosnabjeniye udalennogo obyekta na osnove optimizatsii kl astera VIE: monografiya Yekaterinburg: UrFU, 2013. 100 s.
- 13. Kindryashov A.N., Martyanov A.S., Solomin Ye.V. Elektricheskiye mashini vetroenergeticheskix ustanovok s vertikalnoy osyu vrasheniya / Mejdunarodniy na uchniy jurnal: Alternativnaya energetika i ekologiya. 2013. № 1-2 (118). S. 59-62.
- 14. Semenov V.V. Avtonomnaya sistema elektrosnabjeniya na osnove asinxroni zirovanno sinxronnogo generatora: Avtoreferat diss... kand. texn. nauk. Ufimskiy Gosudarstvenniy aviatsionniy texnicheskiy universitet, Ufa, 2008. 19 s.